Article

Weak Links to Differentiate Weak Bonds: Size-Selective Response of #-Conjugated Macrocycle Gels to Ammonium Ions

Suk-il Kang, Milim Lee, and Dongwhan Lee

J. Am. Chem. Soc., **Just Accepted Manuscript** • DOI: 10.1021/jacs.9b01002 • Publication Date (Web): 19 Mar 2019

Weak Links to Differentiate Weak Bonds: Size-Selective Response of π-Conjugated Macrocycle Gels to Ammonium Ions

Suk-il Kang, Milim Lee, and Dongwhan Lee*

Department of Chemistry, Seoul National University, 1 Gwanak-ro, Gwanak-gu, Seoul 08826, Korea

ABSTRACT: Molecular-level host–guest interactions can drive gel-to-sol phase transitions of the bulk material. Using supramolecular gels constructed from π-conjugated aza-crown macrocycles, we have investigated the effects of guest chemical structures on the kinetics of gel disassembly. While ammonium ions bind only weakly to the individual macrocycles in solution, gel-to-sol transitions of self-assembled macrocycles occur readily under ambient conditions. This net signal amplification process was monitored conveniently by time-dependent spectroscopic studies to reveal a straightforward correlation between the response rate and shape/size of the guest species. Well-designed weak links thus respond to subtle differences in weak bonds, and translate them into visually discernible macroscopic signaling events.

INTRODUCTION

Supramolecular gels are two-component materials in which gelating molecules form insoluble networks that trap solvent molecules inside. If the non-covalent interactions that help maintain the crisscrossing molecular networks can be weakened by external stimuli, such as heat, light, or chemicals, a dramatic gel-to-fluid transition (= degelation) occurs.[1–9] A detailed understanding of the molecular mechanism that underpins such macroscopic change should guide rational design of supramolecular gels as stimuli-responsive materials for chemical sensing,[4–5,10–17] drug delivery,[2,18–20] and reaction control.[8,21] In this paper, we disclose the chemistry of luminescent supramolecular gels of π-conjugated aza-crown macrocycle **M1** (Figure 1) which display size-selective response to various ammonium ions in solution.

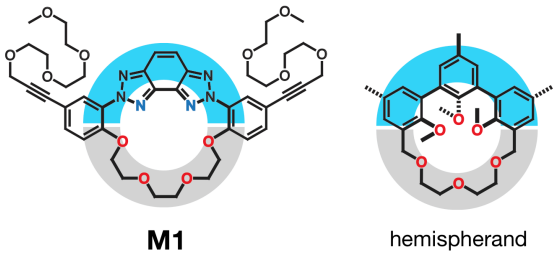

Figure 1. Chemical structures of **M1** (this work) and Cram's hemispherand[22,23] having rigid aromatic-rich hemisphere (in blue) and polar aliphatic-rich flexible hemisphere (in gray).

The host–guest interaction of macrocyclic receptors and ionic species is a textbook example of supramolecular chemistry.[24–26] A large body of binding studies already exist in literature that identify size and shape complementarity as a key factor for tight complexation in solution.[24,27–32] Within this context, it is surprising that this intuitive size differentiation model, often termed as the "hole-size fitting",[24–26,33] has hardly been established in a quantitative manner for supramolecular gels. Previous works on gelating macrocycles focused primarily on the demonstration of guest-induced gel-to-sol transitions.[13–15,34–38] While such visually discernible phase changes could serve as straightforward signaling events, the experimental setup provides only binary information of "to-gel" or "not-to-gel". No quantitative information could be obtained that reflects molecular-level structural variations of the guest species.

BACKGROUND AND DESIGN PRINCIPLES

Preorganization of Crescent-Shaped π-Conjugation. Our entry into the chemistry of π-conjugated aza-crown ether ligands was prompted by the X-ray structure of **1** (Figure 2), prepared initially as a model compound for aromatic foldamers that we recently reported.[39] A contiguous fused array of five-, six-, and five-membered rings in the bis(triazolo)benzene core of **1** nicely defines a crescent-shaped turn motif to support two *N*-aryl substituents that face across the concave side of the molecule.

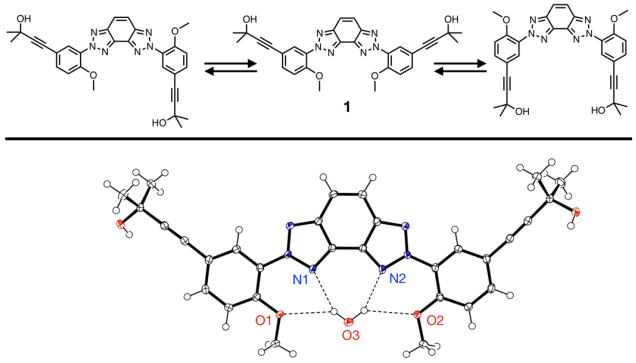

Figure 2. Conformational switching (top) and X-ray structure (bottom; thermal ellipsoids at the 50% probability level) of **1** having a water molecule entrapped within the cavity. See text for key interatomic distances involved in hydrogen bonding (dashed lines).

Even with a finite number of freely rotatable bonds, however, **1** could still adopt at least three different conformations (Figure 2, top) when brought into co-planarity to maximize π-conjugation. A serendipitous co-crystallization with a water molecule, however, produced a single conformer in the solid state (Figure 2, bottom), in which a converging array of $N_{triazole}\cdots H–O_{water}$ ($d_{N\cdots O}$ = 2.942(2)–3.010(2) Å) and $O_{ether}\cdots H–O_{water}$ ($d_{O\cdots O}$ = 3.240(2)–3.247(2) Å) hydrogen bonds function as conformational lock. With H_2O serving as a guest, the two methoxy groups of **1** now point toward the concave side of the molecule. A simple molecular modeling suggested that the crystallographically determined $O_{ether}\cdots O_{ether}$ interatomic distance of 6.445(2) Å here could be spanned by $–(CH_2CH_2O)_n–$ linker groups with n = 2 or 3, without introducing severe steric constraints.

A synthetic scheme was thus devised to strap two separate ether groups into a single crown ether skeleton to build hemi-rigid aza-crown ethers **M1** and **M2** shown in Scheme 1. Built upon rigid π-conjugated platform and flexible oligoether groups, these molecules are reminiscent of the classical hemispherand of Cram (Figure 1),[22,23] although the latter macrocycle has all-oxygen donor atoms.

Scheme 1. Synthetic Routes to Macrocycles M1 and M2, and Acyclic Derivative L

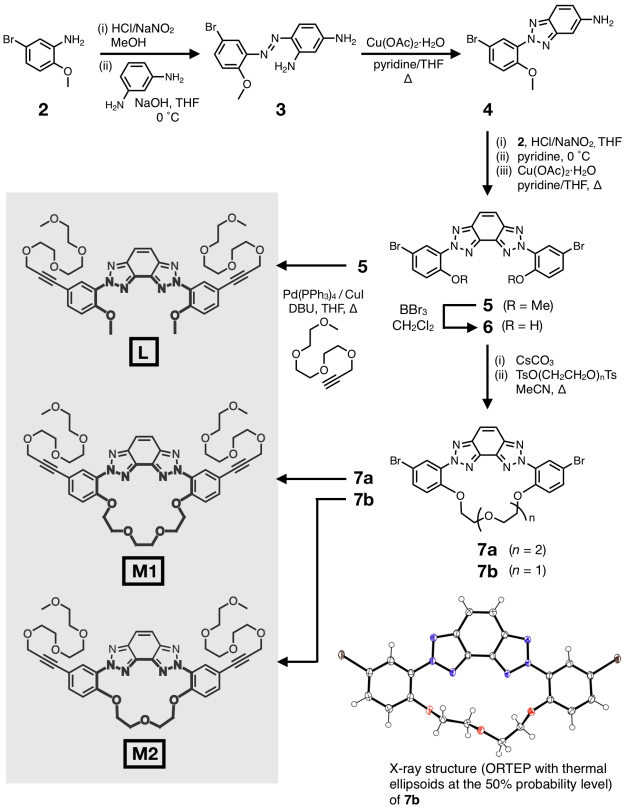

RESULTS AND DISCUSSION

Modular Synthesis of Aza-Crown Macrocycles. As summarized in Scheme 1, our synthesis commenced with **2**, which was subjected to a azo coupling and copper(II)-mediated oxidative cyclization reaction sequences to install the first triazole unit. A second round of azo coupling and cyclization reaction completed the construction of crescent-shaped bis(triazolo)benzene π-skeleton of **5**. Demethylation with BBr_3 converted **5** to **6**, which was divided into two separate reaction batches and subjected to intramolecular cyclization reactions using bistosylated tri- and biethyleneglycol to produce **7a** and **7b**, respectively. The single-crystal X-ray structure of **7b** unambiguously established the desired connectivity. The exceptionally high yield (91%) of the **6**-to-**7a** conversion seems to benefit from the template effect of the cesium ion delivered as carbonate salt. No cyclization product was obtained when lithium carbonate was used as a base under otherwise identical reaction conditions. To improve the solubility of aromatic-rich macrocycles in polar solvents, oligoether tethering groups were installed by Sonogashira–Hagihara coupling to prepare **M1** and **M2** (Scheme 1). An open-chain analogue **L** was prepared directly from **5** in a similar manner.

Supramolecular Gelation: Structure Dependence. Even with the assistance of polar tethering groups, macrocycle **M1** remains insoluble in EtOH at r.t. Upon increasing the temperature to > 45 ˚C, however, the suspension becomes clear, and turns into an opaque gel upon cooling to r.t. This heating–cooling cycle can be repeated to drive reversible sol–gel phase switching (Figure 3a), which is a characteristic thermal behavior of supramolecular gels.[1,40] The morphology of the dried gel, as studied by SEM imaging (Figure 3b), reveals network structures with void spaces.

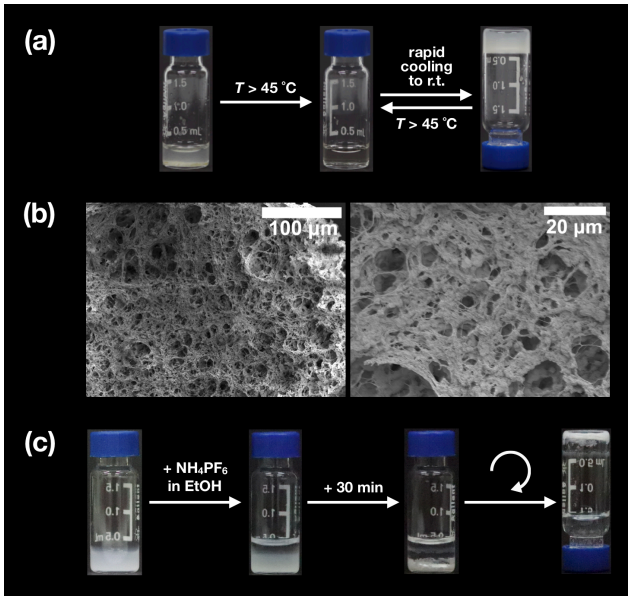

Figure 3. (a) Thermally induced gelation and degelation of **M1** in EtOH. (b) SEM images of dried gel (8 wt%) of **M1**. (c) Chemically induced degelation of **M1** by treatment of ammonium ion at T = 25 ˚C.

In stark contrast, structural analogues of **M1** having smaller macrocycle cavity (**M2**) or unlinked ether groups (**L**) do not produce gel-like structures when subjected to similar thermal treatment conditions; cooling the heated mixture produced only precipitates (Figure 4). It makes intuitive sense that structural rigidification through macrocyclization should help planarize the π-extended molecular core for better self-association through intermolecular contact.[11,41–43] This simplified interpretation, however, fails to explain why **M1** and **M2**, which differ only by the length of the oligoether strap, display such a contrasting gelation behavior (Figure 4b vs Figure 4c).

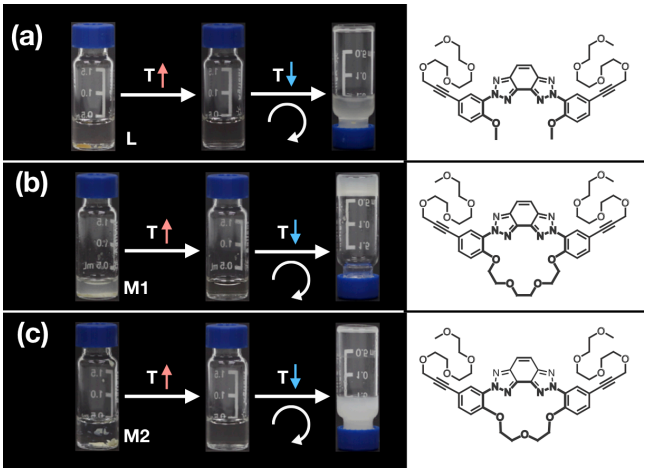

Figure 4. Vial inversion tests on EtOH solution samples (2 wt%) of (a) **L**, (b) **M1**, and (c) **M2** to compare gelation properties.

A DFT computational study was thus carried out to investigate the conformational preference of each molecule. As shown in Figure 5, the geometry-optimized DFT model of **M2** (with the peripheral tethers removed) overlaps nicely with the crystallographically determined structure of **7b** (Scheme 1) which shares identical aza-crown core. However, an increase in the length of the oligoether strap from **M2** to **M1** resulted in a significant canting of the *N*-phenyl rings away from the bis(triazolo)benzene plane (Figure 5, light blue) with computed dihedral angles of 30˚ and 49˚ for **M1**, compared with 13˚ and 35˚ for **M2**. Such a large deviation from co-planarity could have profound impacts on intermolecular π–π stacking, although it remains to be answered how such molecular-level conformational twisting would translate to macroscopic gelation behavior (Figure 4).

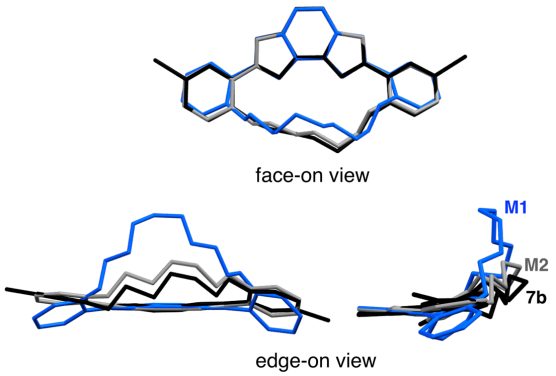

Figure 5. Capped-stick representations of the X-ray structure of **7b** (black) overlaid with DFT (B3LYP/6-31G(d) level) computational models of **M1** (light blue) and **M2** (gray), in which oligoether tethering groups have been removed.

While the underlying molecular mechanism of self-assembly is yet to be elucidated, the markedly different gelation behavior of **M1**, **M2**, and **L** (Figure 4), all sharing identical π-conjugated molecular backbone and peripheral oligoether tethers, points toward the importance of the central macrocyclic cavity in this process. We thus proceed to investigate the possibility of using host–guest chemistry of aza-crown ether to modulate supramolecular gelation of **M1** and find practical applications.

Chemically Induced Gel–Sol Transition: Size-Selective Response to Ammonium Ions. Selective encapsulation of cationic species is the hallmark of crown ether host–guest chemistry.[24,27–28] When the free-standing gel of **M1** was treated with a saturated EtOH solution of NH_4PF_6, degelation occurred at r.t. (Figure 3c). To gain a quantitative understanding of this process, a simple experimental setup was devised. As shown in Figure 6a, the bottom of a dual-path UV–vis quartz cell having a narrow sample compartment was loaded with a fixed amount (0.35 mL) of gel, which was layered with EtOH solvent (0.35 mL) as a buffer to minimize physical agitation during the addition of guest solution as the topmost layer.

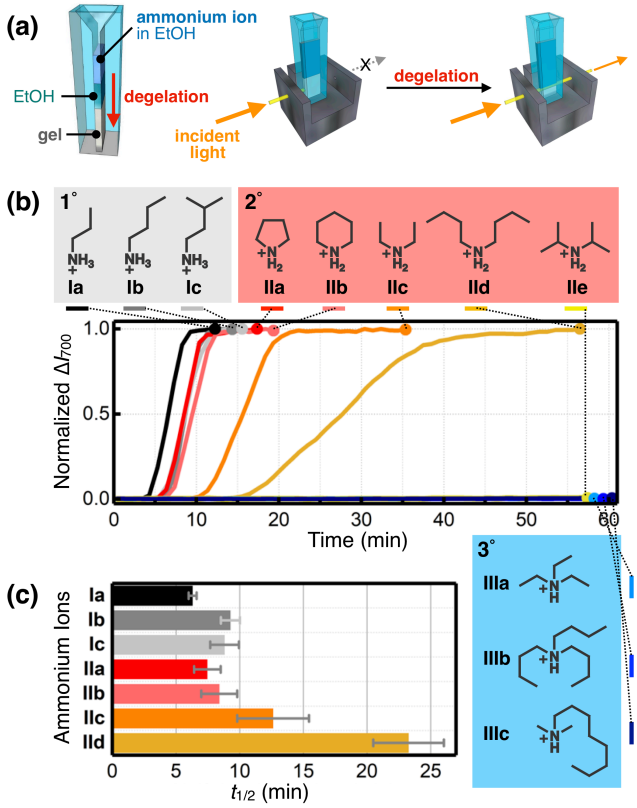

Figure 6. (a) A schematic diagram of UV–vis measurement setup to follow time-dependent gel-to-sol transition of **M1**. (b) Plots of light intensity at λ = 700 nm (normalized to the maximum value, $I_{700,max}$, of each sample) vs time. For samples that show no change in detected light intensity (**IIe**, **IIIa**, **IIIb**, and **IIIc**), normalization was carried out by dividing the raw data with the average $I_{700,max}$ value of the rest of the samples. (c) Structure-dependent degelation rates quantified as $t_{1/2}$ (= time required to reach $I_{700} = 0.5I_{700,max}$). For each sample, measurements were carried out three times under identical conditions to determine the average $t_{1/2}$ value and error bar.

Due to the opaque nature of the gel, the intensity of the incident light at λ = 700 nm passing through the sample is negligible, as monitored by a portable UV–vis spectrometer with fiber optic cables. With the progress of degelation, however, collapse of the opaque molecular network and release of optically transparent **M1** (i.e. having no absorption at λ = 700 nm in solution) clears the beam path, resulting in a sharp rise in the detected light intensity over time (Figure 6b). By plotting time-dependent changes of I_{700}, the degelation process can be

monitored under controlled experimental conditions for direct side-by-side comparison, as shown in Figure 6b.

A series of organic ammonium ions were prepared as PF_6^- salts,[44] and deployed for time-dependent measurements. As shown in Figure 6c, primary ammonium and most of the secondary ammonium elicited structural collapse of the gel. For a quantitative measure, the experimentally determined $t_{1/2}$ values are compared for the subsets of ammonium ions screened (Figure 6c). Among the primary ammonium ions that we screened, longer alkyl chain slows down the response rate (**Ia** vs **Ib** and **Ic**), but increase in the steric bulk at the chain-end position has negligible effects (**Ib** vs **Ic**). A similar trend was observed for the secondary ammonium ions, with longer chains resulting in slower degelation (**IIc** vs **IId**). At the same time, alleviation of the steric congestion around the nitrogen atom through cyclization dramatically accelerates the kinetics of gel collapse (**IIa** vs **IIc**). Intriguingly, comparable $t_{1/2}$ values were observed for secondary ammonium **IIa** and **IIb** having five- and six-membered ring structures, respectively, which, in fact, are as reactive as the primary ammonium **Ib** and **Ic**. Moving in the opposite direction, an increase in steric bulk around the nitrogen atom (**IIe**) completely shut down the degelating capability. With tertiary ammonium ions **IIIa**, **IIIb**, and **IIIc,** as the sterically most crowded subset, no degelation occurred.

Our experimental results implicate that the steric bulk of ammonium ions is a primary determinant of the degelating reactivity. In so much as the chemical structure of macrocyclic core dictates the gelating property of **M1** (Figure 4), access to this cavity by ionic guests seems to be critical to reversing this process (Figure 6). We postulate that complexation of ammonium group by aza-crown ether unit of **M1** would disrupt close intermolecular contacts sustaining the gel network. From the experimentally determined overall trend of 1° > 2° > 3° ammonium ions to facilitate the degelation process, a conceptual linkage could be drawn to the hole-size effect in host–guest chemistry: larger ions do not fit well into the receptor cavity and thus become less effective as degelating agent.

Ammonium Binding by Individual Molecular Receptors in Solution. If the molecular-level size match determines macroscopically observed disassembly rates, how strongly does **M1** bind to an ammonium ion? To address this question, we proceeded to carry out ^{1}H NMR titration studies. To avoid complications from overlapping proton resonances of the oligoether tethers and the crown ether core, compound **8** (Scheme 2) was employed as a simpler model of **M1**.

Scheme 2. Synthetic Routes to Model Macrocycle and Acyclic Analogue

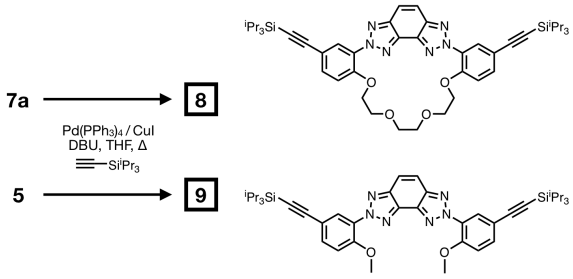

As shown in Figure 7, treatment of **M1** with an increasing amount of NH_4^+, delivered as a PF_6^- salt in acetone-d_6, resulted in systematic downfield shifts of the resonances from the ethylene glycol strap. Apparently, binding of the cationic guest induces deshielding around the cavity region, whereas spectral patterns from the rest of the molecule, including the aromatic region, remain essentially invariant (Figure S1). The ^{1}H NMR titration data shown in Figure 7 was fitted with a 1:1 binding isotherm (Figure S2) to determine the association constant of K_a = 12.68±0.05 M^{-1} for NH_4^+ at T = 25 °C. Spectral titration with K^+ afforded K_a = 9.84±0.04 M^{-1} (Figures S2 and S3).

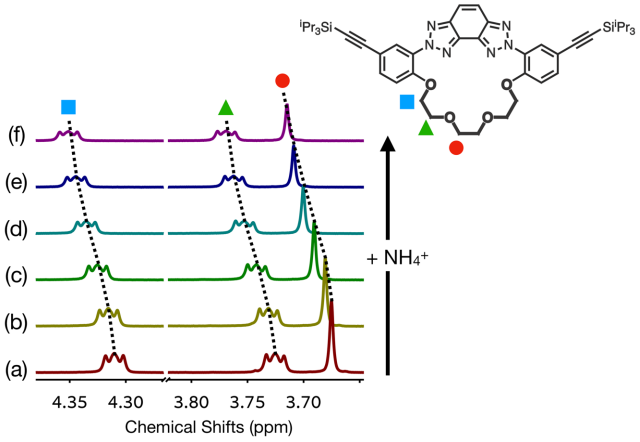

Figure 7. Partial ^{1}H NMR spectra of **8** in acetone-d_6 obtained in the presence of (a) 0, (b) 2, (c) 6, (d) 12, (e) 20, and (f) 28 equiv of NH_4PF_6 at T = 25 °C.

For the acyclic analogue **9** (Scheme 2), however, no spectral shifts were observed upon titration with either NH_4^+ (Figure S4) or K^+ (Figure S5) under similar conditions. This findings support the notion that despite structural preorganization to present the [*N*,*N*]-bidentate donor motif, (i) crescent-shaped bis(triazole)benzene π-backbone by itself is not sufficient, and (ii) conformational lock by oligoether strap is needed to achieve measurable binding affinities toward cationic guests.

Even with the assistance of macrocyclization, the experimentally determined binding constants of ~10 M^{-1} for NH_4^+ or K^+ still lie toward the lower end of typical aza-crown receptors, which usually show K_a = 40–45000 M^{-1}.[27,45] Unlike conventional *N*-donors, the sp^2-nitrogen atoms of the triazole ring (with three electronegative nitrogen atoms constituting the five-membered aromatic ring) are poor donors, which rarely bind to electron-deficient guests in the absence of negatively-charged ancillary groups nearby.[46–49] As such, the weak interaction between the aza-crown cavity of **8** (and therefore **M1**) and ammonium ion is not surprising. What is quite remarkable, however, is the ability of the self-assembled gel of **M1** to amplify such low-affinity binding event, and translate it to macroscopically observed phase-changes that can distinguish even subtle steric differences around the charge center (Figure 6). In retrospect, it makes perfect sense that one needs to use weak interactions in order to measure weak forces, although this simple and intuitive concept seems to have hardly been exploited for ion-responsive supramolecular gels before.

Fluorescence Turn-On Detection by Ammonium-Triggered Release of Entrapped Fluorophores. One notable feature of triazoloarene-based π-conjugation is strong fluorescence emission, which we previously exploited for

reaction-based detection of transition metal ions,[50–51] and intramolecular resonance energy transfer.[52] As a bis(triazolo)benzene derivative, **M1** shows intense (Φ_F = 36%; in $CHCl_3$) emission at λ_{max} = 390 nm (Figure S6) in solution, which prompted us to devise a simple experimental setup as proof-of-concept of target-specific fluorescence enhancement response.

A fluorimeter cell was coated with a small amount (0.1 mL) of **M1**-gel film at the bottom, and filled with EtOH (3 mL). With the fluorophores entrapped as the gelating network, no fluorescence was observed upon excitation of the solution at λ = 365 nm. Upon addition of γ-amminobutyric acid (GABA; 0.3 mL of 1.0 M solution in H_2O:ethanol = 1:3, v/v) as a model analyte, which functions as inhibitory neurotransmitter in biological systems, a sharp rise in the solution fluorescence was observed within 4 min (Figure 8).

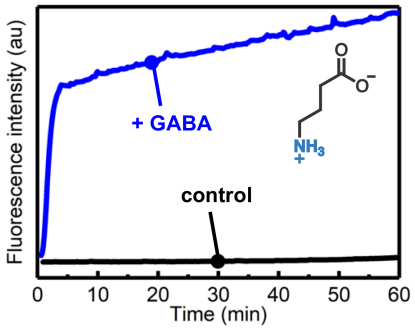

Figure 8. Time-dependent changes in the fluorescence intensity at λ = 400 nm upon treatment of **M1**-gel with GABA (shown as its zwitterionic form). See text for experimental conditions.

A gradual increase in the emission occurred subsequently with further release of the entrapped fluorophore; the signal intensity remained undiminished. Control studies using solvent-only setup showed essentially no changes in the fluorescence intensity, which unambiguously establishes the validity of our design concept.

In typical displacement assays in solution phase, competitive binding of the analyte to the pre-complexed host–indicator pair sets off the signaling event.[53,54] For our system, a single-component supramolecular gel serves the role of the latent host–indicator complex, which, upon encountering the target analyte, rapidly disintegrates and releases its emissive molecular components as the signal output (Figure S7).

SUMMARY AND OUTLOOK

Our studies on new hemispherand-like aza-crown macrocycles have established (i) critical functional role of cavity size for supramolecular gelation; (ii) hole-size effects in guest-induced gel-to-sol transition; (iii) fluorescence turn-on signaling by degelation and release of light-emitting building blocks. Despite inherently weak binding affinity to cationic species at the molecular level, gelated macrocycle can distinguish the size and shape of alkyl ammonium ions through different degelation kinetics.

Non-covalent cross-linking inevitably creates weak links within supramolecular gels. We have demonstrated that such weak links can be used advantageously to tell subtle differences in weak bonds in host–guest chemistry. Efforts are currently underway in our laboratory to expand the scope of this chemistry to different types of stimuli-responsive gels for applications in chemical detection and controlled release.

ASSOCIATED CONTENT

Supporting Information

The Supporting Information is available free of charge on the ACS Publications website.

Synthesis and characterization; additional spectroscopic data (PDF)
X-ray crystallographic data (CIF)

AUTHOR INFORMATION

Corresponding Author

*dongwhan@snu.ac.kr

Notes

The authors declare no competing financial interest.

ACKNOWLEDGMENT

This work was supported by the Basic Research Grant (2017R1A2B2006605) and Creative Materials Discovery Program (2017M3D1A1039558) through the National Research Foundation of Korea (NRF). S.K. thanks the Fellowship for Fundamental Academic Fields from SNU.

REFERENCES

(1) Sangeetha, N. M.; Maitra, U., Supramolecular Gels: Functions and Uses. *Chem. Soc. Rev.* **2005**, *34*, 821–836.

(2) Truong, W. T.; Su, Y.; Meijer, J. T.; Thordarson, P.; Braet, F., Self-Assembled Gels for Biomedical Applications. *Chem. Asian. J.* **2011**, *6*, 30–42.

(3) Goh, C. Y.; Mocerino, M.; Ogden, M. I., Macrocyclic Gelators. *Supramol. Chem.* **2013**, *25*, 555–566.

(4) Segarra-Maset, M. D.; Nebot, V. J.; Miravet, J. F.; Escuder, B., Control of Molecular Gelation by Chemical Stimuli. *Chem. Soc. Rev.* **2013**, *42*, 7086–7098.

(5) Qi, Z.; Schalley, C. A., Exploring Macrocycles in Functional Supramolecular Gels: From Stimuli Responsiveness to Systems Chemistry. *Acc. Chem. Res.* **2014**, *47*, 2222–2233.

(6) Okesola, B. O.; Smith, D. K., Applying Low-Molecular Weight Supramolecular Gelators in an Environmental Setting – Self-Assembled Gels as Smart Materials for Pollutant Removal. *Chem. Soc. Rev.* **2016**, *45*, 4226–4251.

(7) Draper, E. R.; Adams, D. J., Low-Molecular-Weight Gels: The State of the Art. *Chem* **2017**, *3*, 390–410.

(8) Fang, W.; Zhang, Y.; Wu, J.; Liu, C.; Zhu, H.; Tu, T., Recent Advances in Supramolecular Gels and Catalysis. *Chem. Asian. J.* **2018**, *13*, 712–729.

(9) Du, X.; Zhou, J.; Shi, J.; Xu, B., Supramolecular Hydrogelators and Hydrogels: From Soft Matter to Molecular Biomaterials. *Chem. Rev.* **2015**, 115, 13165–13307.

(10) Ge, Z.; Hu, J.; Huang, F.; Liu, S., Responsive Supramolecular Gels Constructed by Crown Ether Based Molecular Recognition. *Angew. Chem., Int. Ed.* **2009**, *48*, 1798–1802.

(11) Krieg, E.; Shirman, E.; Weissman, H.; Shimoni, E.; Wolf, S. G.; Pinkas, I.; Rybtchinski, B., Supramolecular Gel Based on a Perylene Diimide Dye: Multiple Stimuli Responsiveness, Robustness, and Photofunction. *J. Am. Chem. Soc.* **2009**, *131*, 14365–14373.

(12) Dong, S.; Luo, Y.; Yan, X.; Zheng, B.; Ding, X.; Yu, Y.; Ma, Z.; Zhao, Q.; Huang, F., A Dual-Responsive Supramolecular Polymer Gel Formed by Crown Ether Based Molecular Recognition. *Angew. Chem. Int., Ed.* **2011**, *50*, 1905–1909.

(13) Dong, S.; Zheng, B.; Xu, D.; Yan, X.; Zhang, M.; Huang, F., A Crown Ether Appended Super Gelator with Multiple Stimulus Responsiveness. *Adv. Mater.* **2012**, *24*, 3191–3195.

(14) Qi, Z.; Malo de Molina, P.; Jiang, W.; Wang, Q.; Nowosinski, K.; Schulz, A.; Gradzielski, M.; Schalley, C. A., Systems Chemistry: Logic Gates Based on the Stimuli-Responsive Gel–Sol Transition of a Crown Ether-Functionalized Bis(Urea) Gelator. *Chem. Sci.* **2012**, *3*, 2073–2082.

(15) Yan, X.; Xu, D.; Chi, X.; Chen, J.; Dong, S.; Ding, X.; Yu, Y.; Huang, F., A Multiresponsive, Shape-Persistent, and Elastic Supramolecular Polymer Network Gel Constructed by Orthogonal Self-Assembly. *Adv. Mater.* **2012**, *24*, 362–369.

(16) Zheng, B.; Wang, F.; Dong, S.; Huang, F., Supramolecular Polymers Constructed by Crown Ether-Based Molecular Recognition. *Chem. Soc. Rev.* **2012**, *41*, 1621–1636.

(17) Dong, S.; Zheng, B.; Wang, F.; Huang, F., Supramolecular Polymers Constructed from Macrocycle-Based Host–Guest Molecular Recognition Motifs. *Acc. Chem. Res.* **2014**, *47*, 1982–1994.

(18) Vemula, P. K.; Cruikshank, G. A.; Karp, J. M.; John, G., Self-Assembled Prodrugs: An Enzymatically Triggered Drug-Delivery Platform. *Biomaterials* **2009**, *30*, 383–393.

(19) Zhao, F.; Ma, M. L.; Xu, B., Molecular Hydrogels of Therapeutic Agents. *Chem. Soc. Rev.* **2009**, *38*, 883–891.

(20) Liu, Y.; Shi, B.; Wang, H.; Shangguan, L.; Li, Z.; Zhang, M.; Huang, F., Construction of Metallacage-Cored Supramolecular Gel by Hierarchical Self-Assembly of Metal Coordination and Pillar[5]Arene-Based Host-Guest Recognition. *Macromol. Rapid Commun*. **2018**, *39*, 1800655.

(21) Schoonen, L.; van Hest, J. C., Compartmentalization Approaches in Soft Matter Science: From Nanoreactor Development to Organelle Mimics. *Adv. Mater.* **2016**, *28*, 1109–1128.

(22) Koenig, K. E.; Lein, G. M.; Stuckler, P.; Kaneda, T.; Cram, D. J., Host–Guest Complexation. 16. Synthesis and Cation Binding Characteristics of Macrocyclic Polyethers Containing Convergent Methoxyaryl Groups. *J. Am. Chem. Soc.* **1979**, *101*, 3553−3566.

(23) Cram, D. J.; Lein, G. M., Host–Guest Complexation. 36. Spherand and Lithium and Sodium Ion Complexation Rates and Equilibria. *J. Am. Chem. Soc.* **1985**, *107*, 3657–3668.

(24) Steed, J. W.; Atwood, J. L., *Supramolecular Chemistry*. 2nd ed.; Wiley: Chichester, 2009.

(25) Lehn, J. M., Supramolecular Chemistry. Concepts and Perspectives. Wiley-VCH: Weinheim, 1995.

(26) Schneider, H.-J.; Yatsimirsky, A. K., *Principles and Methods in Supramolecular Chemistry*. Wiley: Chechester, 2000.

(27) Christensen, J. J.; Eatough, D. J.; Izatt, R. M., The Synthesis and Ion Bindings of Synthetic Multidentate Macrocyclic Compounds. *Chem. Rev.* **1974**, *74*, 351–384.

(28) Lehn, J. M.; Sauvage, J. P., Cryptates. XVI. [2]-Cryptates. Stability and Selectivity of Alkali and Alkaline-Earth Macrobicyclic Complexes. *J. Am. Chem. Soc.* **1975**, *97*, 6700–6707.

(29) Danil de Namor, A. F.; Cleverley, R. M.; Zapata-Ormachea, M. L., Thermodynamics of Calixarene Chemistry. *Chem. Rev.* **1998**, *98*, 2495–2526.

(30) Del Valle, E. M. M., Cyclodextrins and Their Uses: A Review. *Process Biochem.* **2004**, *39*, 1033–1046.

(31) Assaf, K. I.; Nau, W. M., Cucurbiturils: From Synthesis to High-Affinity Binding and Catalysis. *Chem. Soc. Rev.* **2015**, *44*, 394–418.

(32) Ogoshi, T.; Yamagishi, T. A.; Nakamoto, Y., Pillar-Shaped Macrocyclic Hosts Pillar[*n*]Arenes: New Key Players for Supramolecular Chemistry. *Chem. Rev.* **2016**, *116*, 7937–8002.

(33) Schneider, H.-J.; Yatsimirsky, A. K., Selectivity in Supramolecular Host–Guest Complexes. *Chem. Soc. Rev.* **2008**, *37*, 263–277.

(34) Liu, J.; Chen, G.; Guo, M.; Jiang, M., Dual Stimuli-Responsive Supramolecular Hydrogel Based on Hybrid Inclusion Complex (HIC). *Macromolecules* **2010**, *43*, 8086–8093.

(35) Sobczuk, A. A.; Tamaru, S.; Shinkai, S., New Strategy for Controlling the Oligothiophene Aggregation Mode Utilizing the Gel-to-Sol Phase Transition Induced by Crown-Alkali Metal Interactions. *Chem. Commun.* **2011**, *47*, 3093–3095.

(36) Chen, L.; Tian, Y.-K.; Ding, Y.; Tian, Y.-J.; Wang, F., Multistimuli Responsive Supramolecular Cross-Linked Networks on the Basis of the Benzo-21-Crown-7/Secondary Ammonium Salt Recognition Motif. *Macromolecules* **2012**, *45*, 8412–8419.

(37) Qi, Z.; Wu, C.; Malo de Molina, P.; Sun, H.; Schulz, A.; Griesinger, C.; Gradzielski, M.; Haag, R.; Ansorge-Schumacher, M. B.; Schalley, C. A., Fibrous Networks with Incorporated Macrocycles: A Chiral Stimuli-Responsive Supramolecular Supergelator and Its Application to Biocatalysis in Organic Media. *Chem. Eur. J.* **2013**, *19*, 10150–10159.

(38) Qi, Z.; Traulsen, N. L.; Malo de Molina, P.; Schlaich, C.; Gradzielski, M.; Schalley, C. A., Self-Recovering Stimuli-Responsive Macrocycle-Equipped Supramolecular Ionogels with Unusual Mechanical Properties. *Org. Biomol. Chem.* **2014**, *12*, 503–510.

(39) Kim, S.; Castillo, H. D.; Lee, M.; Mortensen, R. D.; Tait, S. L.; Lee, D., From Foldable Open Chains to Shape-Persistent Macrocycles: Synthesis, Impact on 2D Ordering, and Stimulated Self-Assembly. *J. Am. Chem. Soc.* **2018**, *140*, 4726–4735.

(40) Hanabusa, K.; Suzuki, M., Development of Low-Molecular-Weight Gelators and Polymer-Based Gelators. *Polym. J.* **2014**, *46*, 776–782.

(41) Bhosale, S. V.; Jani, C. H.; Langford, S. J., Chemistry of Naphthalene Diimides. *Chem. Soc. Rev.* **2008**, *37*, 331–342.

(42) Zang, L.; Che, Y.; Moore, J. S., One-Dimensional Self-Assembly of Planar π-Conjugated Molecules: Adaptable Building Blocks for Organic Nanodevices. *Acc. Chem. Res.* **2008**, *41*, 1596–1608.

(43) Xue, P.; Yao, B.; Sun, J.; Zhang, Z.; Lu, R., Emission Enhancement of a Coplanar π-Conjugated Gelator without Any Auxiliary Substituents. *Chem. Commun.* **2014**, *50*, 10284–10286.

(44) Saba, S.; Hernandez, R.; Choy, C. C.; Carta, K.; Bennett, Y.; Bondi, S.; Kolaj, S.; Bennett, C., A Simple and Efficient One-Step Protocol for the Preparation of Alkyl-Substituted Ammonium Tetrafluoroborate and Hexafluorophosphate Salts. *J. Fluorine Chem.* **2013**, *153*, 168–171.

(45) Izatt, R. M.; Bradshaw, J. S.; Nielsen, S. A.; Lamb, J. D.; Christensen, J. J.; Sen, D., Thermodynamic and Kinetic Data for Cation-Macrocycle Interaction. *Chem. Rev.* **1985**, *85*, 271–339.

(46) Butsch, K.; Klein, A.; Nitsche, S.; Stirnat, K.; Hawkett, J. R.; McInnes, E. J.; Bauer, M., Generation and Characterisation of the Phenoxyl-Radical Containing Cu(II) Complex $[Cu(triaz)_2]^+$ (triaz$^-$ = *O,N* Chelating Triazole-Phenolate). *Dalton Trans.* **2012**, *41*, 11464–11475.

(47) Pappuru, S.; Chokkapu, E. R.; Chakraborty, D.; Ramkumar, V., Group IV Complexes Containing the Benzotriazole Phenoxide Ligand as Catalysts for the Ring-Opening Polymerization of Lactides, Epoxides and as Precatalysts for the Polymerization of Ethylene. *Dalton Trans.* **2013**, *42*, 16412–16427.

(48) Chuang, H.-J.; Wu, B.-H.; Li, C.-Y.; Ko, B.-T., Benzotriazole Phenoxide Hafnium Complexes as Efficient Catalysts for the Ring-Opening Polymerization of Lactide: Synthesis, Characterization, and Kinetics of Polymerization Catalysis. *Eur. J. Inorg. Chem.* **2014**, *2014*, 1239–1248.

(49) Stanje, B.; Traar, P.; Schachner, J. A.; Belaj, F.; Mösch-Zanetti, N. C., Iron Catalyzed Oxidation of Benzylic Alcohols to Benzoic Acids. *Dalton Trans.* **2018**, *47*, 6412–6420.

(50) Jo, J.; Lee, H. Y.; Liu, W.; Olasz, A.; Chen, C. H.; Lee, D., Reactivity-Based Detection of Copper(II) Ion in Water: Oxidative Cyclization of Azoaromatics as Fluorescence Turn-on Signaling Mechanism. *J. Am. Chem. Soc.* **2012**, *134*, 16000–16007.

(51) Kim, S.; Jo, J.; Lee, D., Conformationally Distorted π-Conjugation for Reaction-Based Detection of Nickel: Fluorescence Turn-on by Twist-and-Fragment. *Org. Lett.* **2016**, *18*, 4530–4533.

(52) Park, B. G.; Hong, D. H.; Lee, H. Y.; Lee, M.; Lee, D., Multichromophoric π-Conjugation: Modular Design for Gated and Cascade Energy Transfer. *Chem. Eur. J.* **2016**, *22*, 6610–6616.

(53) Wiskur, S. L.; Ait-Haddou, H.; Lavigne, J. J.; Anslyn, E. V., Teaching Old Indicators New Tricks. *Acc. Chem. Res.* **2001**, *34*, 963–972.

(54) Nguyen, B. T.; Anslyn, E. V., Indicator–Displacement Assays. *Coord. Chem. Rev.* **2006**, *250*, 3118–3127.

TOC graphic